Journal of Vibration and Control
http://jvc.sagepub.com/

Mathematical Modeling and Simulation of Thermal Effects in Flexural Microcantilever Resonator Dynamics

G. Nakhaie Jazar
Journal of Vibration and Control 2006 12: 139
DOI: 10.1177/1077546306061555

The online version of this article can be found at:
http://jvc.sagepub.com/content/12/2/139

Published by:

http://www.sagepublications.com

Additional services and information for *Journal of Vibration and Control* can be found at:

Email Alerts: http://jvc.sagepub.com/cgi/alerts

Subscriptions: http://jvc.sagepub.com/subscriptions

Reprints: http://www.sagepub.com/journalsReprints.nav

Permissions: http://www.sagepub.com/journalsPermissions.nav

Citations: http://jvc.sagepub.com/content/12/2/139.refs.html

Downloaded from jvc.sagepub.com at National Science Library CAS on February 27, 2011

Mathematical Modeling and Simulation of Thermal Effects in Flexural Microcantilever Resonator Dynamics

G. NAKHAIE JAZAR
Department of Mechanical Engineering and Applied Mechanics, North Dakota State University, Fargo, ND 58105-5285, USA (Reza.N.Jazar@ndsu.nodak.edu)

(Received 23 March 2005; accepted 14 October 2005)

Abstract: The thermal dependency of material characteristics is an important phenomenon affecting the motion of microresonator systems. Thermal phenomena introduce two main effects: damping due to internal friction, and softening due to the Young's modulus–temperature relationship. Based on reported theoretical and experimental results, we qualitatively model the thermal phenomenon utilizing a Lorentzian function to describe its effect on restoring and damping forces. We present the mathematical modeling of microresonator dynamics and develop effective equations to study the electrically actuated microbeam resonators. In order to study the thermal effects, a linearized model of the microelectromechanical system is adapted. The response of the system at steady-state conditions is developed by employing the averaging perturbation method on the non-dimensionalized form of the equations. Frequency response, resonant frequency and peak amplitude are examined for variation of the dynamic parameters involved.

Key Words: Thermal damping, microelectromechanical systems simulation, microelectromechanical systems dynamics, microbeam, microresonator, mathematical modeling

NOMENCLATURE

a_i	dimensionless parameters of equation of motion
A	effective area of electrode plate
b	width of the microbeam
c	viscous damping rate
c_s	thermal damping force coefficient
C	capacitance
C_p	heat capacity per unit volume
d	gap size
E	Young's modulus
f	external force
f_e	electric force
f_i	inertia force
f_r	bending restoring force

Journal of Vibration and Control, **12(2):** 139–163, 2006 DOI: 10.1177/1077546306061555
©2006 SAGE Publications
Figures 1–9 appear in color online: http://jvc.sagepub.com

Downloaded from jvc.sagepub.com at National Science Library CAS on February 27, 2011

f_{Td}	thermal damping force
f_{Ts}	thermal stiffness force
f_v	viscous damping force
h	dimensionless damping rate, Planck constant
I	cross-sectional second moment of inertia
k_T	thermal stiffness force coefficient
l_T	thermal diffusion length
L	length of microbeam or microcantilever
$\mathcal{L} = x/(1+x^2)$	Lorentzian function
m	effective mass
n	mode shape parameter
Q	quality factor
$r = \omega/\omega_1$	dimensionless excitation frequency
t	time
T	temperature
T_0	uniform temperature
$v = v_i \sin(\omega t)$	alternative excitation voltage
v_p	polarization voltage
w	lateral displacement
x	longitudinal coordinate
y	lateral coordinate, dimensionless lateral displacement
Y	dimensionless amplitude of oscillations at maximum
Z	longitudinal dimensionless coordinate
α	polarization voltage parameter
α_T	thermal expansion coefficient
β	alternative voltage parameter
γ_T	thermal diffusivity
φ	mode shape function
ρ	mass per unit length
ω	frequency of alternative voltage
ω_i	ith resonance frequency
τ_Z	Zener relaxation time
$\xi = a\sqrt{\omega_i/2\gamma_T}$	
ϵ_0	permittivity in vacuum
$\tau = \omega_1 t$	dimensionless time
overdot	$d(\ )/d\tau$

1. INTRODUCTION

The purpose of this paper is to provide a consistent theory for the prediction of the effects of intrinsic dissipation arising from thermoelectricity in dynamic behavior and sensitivity analysis of microresonators. Particular attention will be given to flexural motion of electrically actuated microbeams. This work is a step toward modeling and understanding the fundamental limits of design in small resonating sensors in nanoscale and microscale. The thermal properties of the microbeam material can play a significant role in affecting the

Downloaded from jvc.sagepub.com at National Science Library CAS on February 27, 2011

design and application of microsystems utilizing a microbeam or microcantilever resonator (Karami and Garnich, 2005). The energy loss in a micromechanical resonator is measured in terms of the quality factor, defined as $Q = 2\pi e_0/\Delta e$, where e_0 is the mechanical energy of the resonator and Δe is the energy loss per cycle. The quality factor for a lightly damped single-degree-of-freedom system with damping ratio $\xi \ll 1$ is $Q = 1/(2\xi)$. It is reasonable to assume microsystems are lightly damped, so $Q \gg 1$ (Norris and Photiadis, 2005).

We focus on an analytical approach to the development of a mathematical model for the thermal phenomena and their effects on microelectromechanical systems (MEMS) dynamics. To do this, a linearized model of electrically actuated microbeam resonators will be employed. The effects of thermal phenomena are modeled as an increase in damping and a decrease in stiffness rates, both as a Lorentzian function of excitation frequency. The steady-state frequency–amplitude dependency of the system will be derived utilizing the averaging perturbation method. The developed analytic equation describing the frequency response of the system around resonance can be utilized to examine the dynamics of the system, as well as resonant frequency and peak amplitude.

The application of MEMS has been growing since 1980; however, MEMS and MEMS devices have mainly been designed by trial and error, mainly because most MEMS devices are modeled using weak or simplified analytical tools, resulting in a relatively approximate prediction of performance. As a result, the MEMS design process requires several iterations before the performance requirements of a given device are finally satisfied. However, experimental results depend on the accuracy of the experimental devices and, even more prominently, depend on the skills and knowledge of the experimenter. The finite element method (FEM) software is limited because it is time-consuming, cumbersome, expensive, and uses numerous variables to represent the state of the system, where most of those variables are not important to the designer (Younis, Abdel-Rahman, and Nayfeh, 2003; Younis, 2004). Conversely, the reduced-order models, known as macromodels, need to be expanded and improved as a basis for prediction and optimization of the proposed behavior. Reduced-order models are developed to capture the most significant characteristics of MEMS behavior in a few variables (Nayfeh and Younis, 2004; Younis, 2004).

Microbeam-based sensors and actuators must work at resonance. Resonance is the property of a system to describe an enhanced response at a certain characteristic natural frequency that is solely determined by the parameters of the system. The specific frequency is one where the system retains input energy with minimum loss. Resonance may be observed in any dynamical systems. Typical microresonator devices employ a parallel capacitor, in which one electrode is fixed and the other is allowed to move using some flexibility. The movable electrode, fabricated in the form of a microbeam, microplate, or microcantilever, serves as a mechanical resonator. It is actuated electrically and its motion can be detected by capacitive changes. This motion of the movable electrode can be converted to an electric signal in the capacitance, which is related to the physical quantity being measured (Younis and Nayfeh, 2003).

In this analysis we assume the thermal damping can be high, up to 20% of the equivalent viscous damping of the system. Although the thermal damping is much lower than viscous damping in normal systems, we may assume the microresonator is working in a vacuumed capsule, so the viscous damping is too low and the high relative thermal damping is possible. In addition, we assumed that the rigidity and, hence, the equivalent stiffness of the

Downloaded from jvc.sagepub.com at National Science Library CAS on February 27, 2011

microbeam can be reduced 20% by the thermal effect, which is a very high reduction for the common materials used for microbeams. The finalized equations are dimensionless, so they can be utilized for any specific material and situation.

2. MATHEMATICAL MODELING

2.1. Reduced Model of Microresonators

The electric load and the mechanical restoring forces are the most important forces that govern MEMS dynamics. Electric actuation is achieved by applying a voltage difference between the opposite electrodes of a variable capacitor. The induced electromagnetic force deforms the capacitor until it is balanced by the restoring mechanical force. The electric load is composed of a DC polarization voltage, v_p, and an AC actuating voltage, $v = v_i \sin(\omega t)$. The DC voltage applies an electrostatic force on the microbeam and usually changes the equilibrium position. The polarization voltage has an upper limit called the “collapse” load, beyond which the mechanical restoring force can no longer resist its opposing force (Hsu, 2002).

The one-dimensional electrostatic force, f_e, between two electrodes is

$$f_e = \frac{\varepsilon_0 A \left(v + v_p\right)^2}{2\left(d - w\right)^2}, \qquad v = v_i \sin(\omega t) \tag{1}$$

where $\varepsilon_0 = 8.85 \times 10^{-12}$ AsVm^{-1} is permittivity in vacuum, A is the area of the microplate, and $w = w(x,t)$ is the lateral displacement of the microbeam (Hsu, 2002). The complete microresonator is composed of a beam attached to a microplate as a movable electrode, a ground plane underneath, and one (or more) capacitive transducer electrode(s). To bias and excite the device, a DC bias voltage, v_p, is applied to the resonator while an AC excitation voltage is applied to its underlying ground plate(s). A variable capacitor model on a clamped–clamped microbeam and a microcantilever are illustrated in Figure 1.

When the applied AC excitation has a frequency close to the fundamental resonance frequency of the resonator, the resonator begins to oscillate, creating a time-varying capacitance $C = \varepsilon_0 A/(d - w)$ between the resonator and the electrode. It is usually assumed that the beam length is much greater than the electrode lengths. Therefore, the variation of the beam deflection across the length of the electrodes can be ignored (Nguyen, 1995).

The restoring force of the microbeam is composed of three components: bending, axial force, and mid-plane stretching. However, in this study, only the bending restoring force is considered to emphasize the effects of the thermal phenomenon. Therefore, the restoring force per unit length is only a result of the rigidity of the microbeam and is expressed by

$$f_r = EI \frac{\partial^4 w}{\partial x^4}. \tag{2}$$

The inertia force per unit length of a vibrating microbeam is

Downloaded from jvc.sagepub.com at National Science Library CAS on February 27, 2011

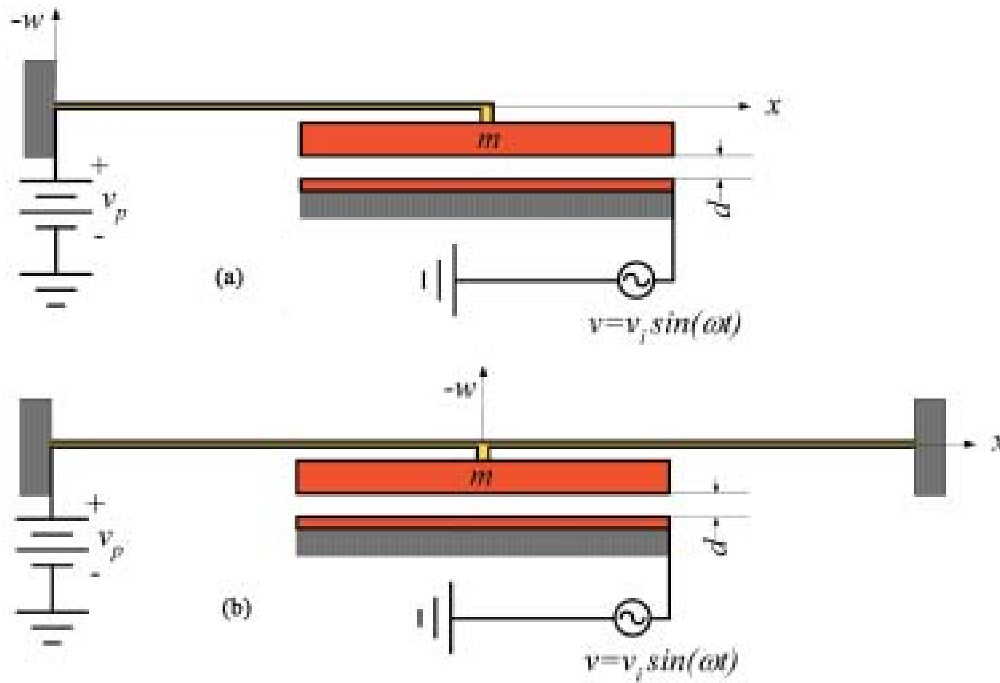

Figure 1. A microcantilever and a clamed–clamped microbeam model of a MEMS and its voltage connections.

$$f_i = \rho \frac{\partial^2 w}{\partial t^2}, \tag{3}$$

where ρ is the mass per unit length of the microbeam.

Damping strongly affects the dynamics, control, performance, and design of MEMS. The influence of damping on the dynamics of MEMS depends on their design and operating conditions. There are several energy dissipation mechanisms in MEMS devices. Air damping, squeezed-film damping, damping due to crystallographic defects, acoustic radiation or thermoelastic damping, internal, structural, intrinsic losses, viscous damping, and acoustic radiation from the supports of the beam (also called anchor or clamping losses) are the most common sources of energy dissipations (Nguyen, 1995; Wang et al., 2000; Younis and Nayfeh, 2003). Among these, the viscous damping force

$$f_v = c \frac{\partial w}{\partial t} \tag{4}$$

is the most important and unavoidable one, where c is the equivalent damping coefficient per unit length of the microbeam. Mostly, damping and dissipation mechanisms are mixed and coupled; however, it is conventional to define an equivalent viscous damping for some of these (Wang et al., 2000).

Downloaded from jvc.sagepub.com at National Science Library CAS on February 27, 2011

2.2. Frequency Dependence of Thermal Noise

Some of the sources of energy loss are considered extrinsic in that they can be altered by changing the design or operating conditions. For example, operating the device in vacuum and designing non-intrusive supports reduces air damping and clamping losses, respectively (Wang et al., 2000; Hsu et al., 2001). However, intrinsic sources of dissipation impose a strict upper limit on the attainable quality factors of resonators.

Thermoelastic damping, also known as “thermomechanical noise,” is the external effect of sound waves traveling through an elastic material, and is a consequence of the microbeam being in thermal equilibrium with its environment. Energy dissipation in the microbeam causes the stored elastomechanical energy to leak away and be converted into heat. It depends on the thermodynamic properties of the material which are functions of temperature. In microresonators, the thermoelastic damping is proportional to frequency; hence, when the principal natural frequency moves up while the size of devices decreases, thermal damping becomes more significant (Lifshitz and Roukes, 2000). Thermoelastic damping also refers to the capacity of a solid to transform the ordered energy of vibration into disordered internal energy. Local adiabatic changes in the mechanical stress generate local temperature changes in thermoelastic solids. In turn, the temperature changes lead to irreversible heat flow and to entropic dissipation. In other words, thermal energy dissipation is caused by irreversible heat flow across the thickness of the microcantilever as it oscillates (Yasumura et al., 2000).

The material linear thermal expansion coefficient $\alpha_T = (1/L)\,(\partial L/\partial T)$ is the macroscopic parameter that couples changes of length (strain) with changes of temperature. The coupling of the strain field to a temperature field provides an energy dissipation mechanism. We call this damping mechanism the “temperature relaxation”, which warms up every vibrating thermoelastic solid, and allows a free system to relax back to rest. Generally, the material of the beam will be softened by heat, resulting in a softening stiffness rate. The relaxation of the thermoelastic solid is achieved through the irreversible flow of heat driven by local temperature gradients produced by a strain field.

Zener was the first researcher to investigate and model the effect of internal frictions in resonating thermoelastic solids, known as thermoelastic damping today (Zener, 1937, 1938a, 1938b, 1948). According to the Zener approximate theory, the thermoelastic damping is significant when the frequency of vibration, ω, satisfies the condition $\omega\tau_Z = 1$, where $\tau_Z = a^2/\left(\pi^2\gamma_T\right)$ is the Zener relaxation time, a is the thickness of the microbeam, and γ_T is the thermal diffusivity of the microbeam material (Zener, Otis, and Nuckolls, 1938). The Zener relaxation time, τ_Z, is related to the quality factor due to the following relationship

$$Q_Z^{-1} = \frac{E\alpha_T^2 T_0}{C_p}\frac{\omega\tau_Z}{1+(\omega\tau_Z)^2},$$

where C_p is the heat capacity per unit volume of the beam material, T_0 is the uniform temperature of the beam, and E is Young’s modulus. In fact, as Zener first demonstrated, the simple expression (5) is the leading term in an infinite series which is well approximated by the single term (Zener, 1937; Norris and Photiadis, 2005). A spring, parallel to a series of spring and damper, is the mechanical model leading to the Zener equation (Saulson, 1990).

A better approximation for equation (5) is provided by Alblas (1961, 1981) and Lifshitz and Roukes (2000) as follows

Downloaded from jvc.sagepub.com at National Science Library CAS on February 27, 2011

$$Q^{-1} = \frac{6E\alpha_T^2 T_0}{C_p}\left(\frac{1}{\xi^2} - \frac{1}{\xi^3}\frac{\sinh\xi + \sin\xi}{\cosh\xi + \cos\xi}\right), \qquad \xi = a\sqrt{\frac{\omega_i}{2\gamma_T}}, \tag{6}$$

where ω_i is the ith natural frequency of the microbeam, and ξ is dimensionless and proportional to $\sqrt{\omega\tau}$. This expression has a maximum at $\xi \simeq 2.225$, equal to $Q^{-1}/\left(E\alpha_T^2 T_0/C_p\right) = 0.494$. Note that the maximum is independent of the dimension of the microbeam. It is a function of temperature, E, α_T, and C_p. The natural frequencies or eigenfrequencies for microbeams in terms of the beam dimensions are $\omega_i = a_i^2\pi^2\sqrt{EI/\left(\rho L^4\right)}$, where I is the area second moment of inertia of the cross-section, and a_i is a number depending on the boundary conditions of the beam (Meirovitch, 1997). Therefore, $\xi^2 = a_i^2\pi^2 b^2/\left(4\sqrt{3}L^2 l_T\right)$, where $l_T = \gamma_T\sqrt{\rho/E}$ is the thermal diffusion length. The values of l_T are measured experimentally for the material of the beam and are tabulated. The analytic equation (5) or (6) can be approximated by the following simpler equation with less than 1% error

$$Q^{-1} = \frac{E\alpha_T^2 T_0}{C_p}\mathcal{L}\left(\omega t\right), \qquad \mathcal{L}\left(x\right) = \frac{x}{1+x^2} \tag{7}$$

where L is the Lorentzian function (Gough, 1968; Lifshitz and Roukes, 2000). The Lorentzian function has been derived and used in thermal-loss analysis, especially in flexural beam resonators by most researchers (Srikar and Senturia, 2002; Yang et al., 2002; Abdolvand et al., 2003; Jeong et al., 2003; De and Aluru, 2004; Fejer et al., 2004; Husman et al., 2004).

For a linear mass–spring–dashpot oscillator, the quality factor Q, is defined by $Q = \sqrt{km}/c$. Therefore, employing equation (6), we introduce a frequency-dependent force

$$f_{Td} = c_T \frac{\omega/\omega_1}{1 + (\omega/\omega_1)^2}\frac{\partial w}{\partial t} \tag{8}$$

to simulate the damping force corresponding to thermal warming up. The coefficient c_T defines the thermal damping per unit length of the microbeam and must be determined experimentally. The thermal damping force introduces a new characteristic within the equation of motion, since it is a function of excitation frequency with a maximum at fundamental resonance frequency. In other words, the thermal damping is modeled by a viscous damping with a Lorentzian frequency-dependent damping coefficient.

The thermoelastic phenomenon also affects the rigidity of the material, since the rigidity is also temperature-dependent. Most engineering materials become softer at higher temperatures. As a microbeam is flexed, one side heats and the other cools. Heat flows to attempt to restore equilibrium, causing the restoring force from the microbeam to relax from its initial value to a smaller equilibrium value (Barmatz and Chen, 1974; Saulson, 1990; Gysin et al., 2004). Since the warming of the microbeam material is Lorentzian frequency-dependent, the effect of stiffness softening of the microbeam is also a frequency-dependent characteristic. So we present a negative function to define this behavior. More specifically, a negative restoring force with stiffness as a Lorentzian function of excitation frequency

$$f_{Ts} = -k_T \frac{\omega/\omega_1}{1 + (\omega/\omega_1)^2} w \tag{9}$$

Downloaded from jvc.sagepub.com at National Science Library CAS on February 27, 2011

determines the drop in linear rigidity stiffness force, $f_r = EI\left(\partial^4 w/\partial x^4\right)$. The breaking frequency of the thermal stiffness softening is also at the fundamental resonance frequency. The softening stiffness coefficient per unit length, k_T, must also be determined experimentally.

2.3. Equation of Motion

The equation describing lateral vibrations of the microbeam can be summarized and simplified to the following equation when the beam's geometry is uniform:

$$\rho\frac{\partial^2 w}{\partial t^2} + c\frac{\partial w}{\partial t} + EI\frac{\partial^4 w}{\partial x^4} + c_T\frac{\omega/\omega_1}{1+(\omega/\omega_1)^2}\frac{\partial w}{\partial t} - k_T\frac{\omega/\omega_1}{1+(\omega/\omega_1)^2}w = \frac{\varepsilon_0 A\left(v+v_p\right)^2}{2\left(d-w_0\right)^2}. \tag{10}$$

We define the following variables to make the equation of motion dimensionless (the parameter n is a constant depending on the mode shape of the microbeam):

$$\tau = \omega_1 t \qquad \omega_1 = \frac{n}{L^2}\sqrt{\frac{EI}{\rho}} \qquad z = \frac{x}{L} \qquad y = \frac{w}{d} \qquad Y = \frac{w_0}{d} \qquad r = \frac{\omega}{\omega_1}$$
$$a_1 = \frac{\varepsilon_0 A L^4}{2n^2 d^3 EI} \qquad a_2 = \frac{cL^2}{n\sqrt{\rho EI}} \qquad a_6 = \frac{c_T L^2}{n\sqrt{\rho EI}} \qquad a_7 = \frac{k_T L^4}{n^2 EI}. \tag{11}$$

Utilizing these parameters, the equation of motion transforms to the following dimensionless equation:

$$\frac{\partial^2 y}{\partial \tau^2} + a_2\frac{\partial y}{\partial \tau} + \frac{\partial^4 y}{\partial z^4} + a_6\frac{r}{1+r^2}\frac{\partial y}{\partial \tau} - a_7\frac{r}{1+r^2}y = a_1\frac{\left(v+v_p\right)^2}{(1-Y)^2}. \tag{12}$$

We apply a separation solution

$$y = Y(\tau)\cdot\varphi(z) \tag{13}$$

where the spatial function $\varphi(z)$ is called the mode shape function, and must satisfy the boundary conditions. By accepting a first harmonic shape function, the temporal function $Y(\tau)$ would then represent the maximum deflection of the microbeam, which is the middle point for symmetric boundary conditions, and the tip point for the microcantilever. For other boundary conditions, the function $Y(\tau)$ must be defined depending on the coordinate system and the appropriate first mode shape.

In the following sections we assume a first harmonic function as the mode shape function for the deflected microbeam. However, prior to this, we show, in the following subsections, that introducing the mode shape parameter n enables us to unify the equation of motion for microcantilevers and symmetric microbeams.

Downloaded from jvc.sagepub.com at National Science Library CAS on February 27, 2011

2.3.1. Clamped–Clamped Microbeam

Considering a clamped–clamped microbeam requires the following boundary conditions:

$$y\left(\frac{1}{2},\tau\right)=y\left(-\frac{1}{2},\tau\right)=0 \qquad \frac{\partial}{\partial z}y\left(\frac{1}{2},\tau\right)=\frac{\partial}{\partial z}y\left(-\frac{1}{2},\tau\right)=0. \tag{14}$$

The following mode shape satisfies the required boundary conditions

$$\varphi(z)=\frac{1}{2}\left[1+\cos\left(2\pi z\right)\right]. \tag{15}$$

Adapting

$$n=2\sqrt{2}\pi^2 \tag{16}$$

and equation (15), we substitute equation (13) into equation (20) to find the temporal differential equation describing the evolution of the temporal function $Y(\tau)$ for a clamped–clamped microbeam:

$$\ddot{Y}+\left(h+a_6\frac{r}{1+r^2}\right)\dot{Y}+\left(1-a_7\frac{r}{1+r^2}\right)Y$$
$$=\frac{1}{(1-Y)^2}\left[(\alpha+\beta)+2\sqrt{2\alpha\beta}\sin\left(r\tau\right)-\beta\cos\left(2r\tau\right)\right] \tag{17}$$

where

$$h=a_2 \qquad \alpha=a_1v_P^2 \qquad 2\sqrt{2\alpha\beta}=2a_1v_Pv_i \qquad \beta=\frac{a_1}{2}v_i^2. \tag{18}$$

2.3.2. Simple–Simple Microbeam

In the case of a simple–simple microbeam, the boundary conditions would be

$$y\left(\frac{1}{2},\tau\right)=y\left(-\frac{1}{2},\tau\right)=0 \qquad \frac{\partial^2}{\partial z^2}y\left(\frac{1}{2},\tau\right)=\frac{\partial^2}{\partial z^2}y\left(-\frac{1}{2},\tau\right)=0. \tag{19}$$

The first harmonic mode shape satisfying the required boundary conditions is

$$\varphi(z)=\cos\left(\pi z\right) \tag{20}$$

and the mode shape parameter is

$$n=\pi^2. \tag{21}$$

Substituting these results into the general equation (12) leads to the same differential equation (17) and describes the dynamic behavior of the temporal function $Y(\tau)$ for a simple–simple

Downloaded from jvc.sagepub.com at National Science Library CAS on February 27, 2011

microbeam. However, the parameters of the simple–simple microbeam are related to the parameters of the clamped–clamped microbeam as defined below

$$\begin{aligned} 8\,(a_1)_{CC} &= (a_1)_{SS} \quad 2\sqrt{2}\,(a_2)_{CC} = (a_2)_{SS} \\ 2\sqrt{2}\,(a_6)_{CC} &= (a_6)_{SS} \quad 8\,(a_7)_{CC} = (a_7)_{SS}\,, \end{aligned} \tag{22}$$

where the subscript CC denotes clamped–clamped, and SS denotes simple–simple.

2.3.3. Microcantilever

A microcantilever is a microbeam with the following boundary conditions.

$$y\,(0,\tau) = 0 \qquad \frac{\partial}{\partial z} y\,(0,\tau) \qquad \frac{\partial^2}{\partial z^2} y\,(1,\tau) = 0 \qquad \frac{\partial^3}{\partial z^3} y\,(1,\tau) = 0. \tag{23}$$

The first harmonic mode shape to satisfy the required boundary conditions in this case is

$$\varphi(z) = 1 - \cos\left(\frac{\pi z}{2}\right) \tag{24}$$

and the mode shape parameter is

$$n = \frac{\pi^2}{4}. \tag{25}$$

Therefore, the required differential equation for the temporal function $Y(\tau)$ related to a microcantilever would be the same equation (17) with new parameters according to the following relations

$$16\,(a_1)_{SS} = (a_1)_C \quad 4\,(a_2)_{SS} = (a_2)_C \quad 4\,(a_6)_{SS} = (a_6)_C \quad 16\,(a_7)_{SS} = (a_7)_C\ , \tag{26}$$

where the subscript C denotes cantilever.

3. LINEARIZED MODEL

In this section we review the linear case of the system with and without polarization. It is possible (and has actually been done by a few researchers) that the nonlinear electrostatic force be expanded in a Taylor series expansion

$$\frac{1}{(1-Y)^2} = 1 + 2Y + 3Y^2 + 4Y^3 + 5Y^4 + 6Y^5 + O(Y^6). \tag{27}$$

Then, depending on the order of acceptable nonlinearities and interested phenomena, different terms are accepted.

Downloaded from jvc.sagepub.com at National Science Library CAS on February 27, 2011

First consider the case in which $v_p = 0$. This is a practical model to eliminate the asymmetric problems caused by shifting the rest point. Eliminating the polarization voltage simplifies the governing equation to

$$\ddot{Y} + \left(h + a_6 \frac{r}{1+r^2}\right)\dot{Y} + \left(1 - a_7 \frac{r}{1+r^2}\right) Y = \frac{\beta}{(1-Y)^2}\left[1 - \cos(2r\tau)\right]. \quad (28)$$

Adapting a linear approximation and ignoring the thermal terms, we convert the equation of motion to a forced Mathieu-type differential equation

$$\ddot{Y} + h\dot{Y} + \left[1 - 2\beta + 2\beta\cos(2r\tau)\right] Y = 2\beta\sin^2(r\tau). \quad (29)$$

Note that thermal effects are linear in Y with frequency-dependent coefficients. Therefore, it is possible to consider the thermal effects even in the linear model, using the following equation

$$\begin{aligned} &\ddot{Y} + \left(h + a_6 \frac{r}{1+r^2}\right)\dot{Y} + \left[\left(1 - a_7 \frac{r}{1+r^2}\right) - 2\beta + 2\beta\cos(2r\tau)\right] Y \\ = \ & 2\beta\sin^2(r\tau). \end{aligned} \quad (30)$$

The difference between models (29) and (30) is the existence of frequency response, since equation (29) does not show a frequency response while model (30) does, as will be shown in the next section.

The dynamics behavior of the microresonator is more interesting when a polarization voltage is present. Assuming that the polarization voltage is less than the collapse voltage, the governing equation of the MEMS to analyze the thermal effects would be

$$\begin{aligned} &\ddot{Y} + \left(h + a_6 \frac{r}{1+r^2}\right)\dot{Y} + \left[\left(1 - a_7 \frac{r}{1+r^2}\right) - 2\beta - 2\alpha \right.\\ + \ & \left. 2\beta\cos(2r\tau) - 4\sqrt{2\alpha\beta}\sin(r\tau)\right] Y = \alpha + 2\beta\sin^2(r\tau) + 2\sqrt{2\alpha\beta}\sin(r\tau). \end{aligned} \quad (31)$$

It is clear that equation (31) reduces to equation (30) by putting $\alpha = 0$.

4. MATHEMATICAL ANALYSIS

In order to find the amplitude of oscillation of the microbeam around resonance and taking care of initial displacement due to polarization, we assume a solution in the following form

$$Y = A_0 + A(\tau)\sin\left[r\tau + \psi(\tau)\right] \quad (32)$$

$$\dot{Y} = A(\tau) r \cos\left[r\tau + \psi(\tau)\right]. \quad (33)$$

This assumption applies provided that

Downloaded from jvc.sagepub.com at National Science Library CAS on February 27, 2011

$$\dot{A}(\tau)\sin[r\tau+\psi(\tau)]+A(\tau)\dot{\psi}(\tau)\cos[r\tau+\psi(\tau)]=0. \tag{34}$$

Substituting equations (32) and (33) into equation (31) leads to the following equation of motion

$$\begin{aligned}
& \left[1-2\alpha-2\beta+2\beta\cos(2r\tau)-4\sqrt{2\alpha\beta}\sin(r\tau)-r\left(r+\dot{\psi}(\tau)\right)\right] \\
\times\ & A(\tau)\left(1+r^2\right)\sin[r\tau+\psi(\tau)]-a_7 rA(\tau)\sin[r\tau+\psi(\tau)] \\
+\ & \left[\left(hA(\tau)+\dot{A}(\tau)\right)r\left(1+r^2\right)+a_6 r^2 A(\tau)\right]\cos[r\tau+\psi(\tau)] \\
-\ & 2\sqrt{2\alpha\beta}(1+2A_0)\left(1+r^2\right)\sin(r\tau)+\beta(1+2A_0)\left(1+r^2\right)\cos(2r\tau) \\
+\ & \left[(1-2\alpha-2\beta)\left(1+r^2\right)-a_7 r\right]A_0-(\beta+\alpha)\left(1+r^2\right)=0.
\end{aligned} \tag{35}$$

Elimination of the secular terms requires that

$$A_0=\frac{(\alpha+\beta)\left(1+r^2\right)}{(1-2\alpha-2\beta)\left(1+r^2\right)-a_7 r}. \tag{36}$$

Equations (34) and (35) make a set of equations to be solved for $A(t)$ and $\psi(t)$. These equations can be decoupled to obtain the following set of equations:

$$\begin{aligned}
\dot{A}(\tau) =\ & \frac{-1}{r}\cos[\varphi(\tau)]\left\{\left(h+\frac{a_6 r}{1+r^2}\right)rA(\tau)\cos[\varphi(\tau)]\right. \\
-\ & \left(2\beta+r^2+2\alpha-1+a_7 r\right)A(\tau)\sin[\varphi(\tau)]+2(1+\beta)A_0 \\
\times\ & \sin[\varphi(\tau)-\psi(\tau)]-2\sqrt{2\alpha\beta}A(\tau)\cos[2\varphi(\tau)-2\psi(\tau)] \\
-\ & 2\sqrt{2\alpha\beta}(2A_0+1)\cos[\psi(\tau)]+\beta A(\tau)\sin[3\varphi(\tau)-2\psi(\tau)] \\
+\ & 2\sqrt{2\alpha\beta}A(\tau)\cos[2\varphi(\tau)-\psi(\tau)]-\beta A(\tau)\sin[\varphi(\tau)-2\psi(\tau)] \\
-\ & \left.(1+2A_0)(\alpha+\beta)+A_0\left(1+\frac{a_7 r}{1+r^2}\right)-\beta\right\}
\end{aligned} \tag{37}$$

$$\begin{aligned}
A(\tau)\dot{\psi}(\tau) =\ & \frac{1}{r\left(1+r^2\right)}\sin[\varphi(\tau)]\left\{\left(h+\frac{a_6 r}{1+r^2}\right)rA(\tau)\cos[\varphi(\tau)]\right. \\
-\ & \left(2\beta+r^2+2\alpha-1+a_7 r\right)A(\tau)\sin[\varphi(\tau)]+2(1+\beta)A_0 \\
\times\ & \cos[2\varphi(\tau)-2\psi(\tau)]-2\sqrt{2\alpha\beta}(2A_0+1)\sin[\varphi(\tau)-\psi(\tau)] \\
-\ & 2\sqrt{2\alpha\beta}A(\tau)\cos[\psi(\tau)]+\beta A(\tau)\sin[3\varphi(\tau)-2\psi(\tau)] \\
+\ & 2\sqrt{2\alpha\beta}A(\tau)\cos[2\varphi(\tau)-\psi(\tau)]-\beta A(\tau)\sin[\varphi(\tau)-2\psi(\tau)] \\
-\ & \left.(1+2A_0)(\alpha+\beta)+A_0\left(1+\frac{a_7 r}{1+r^2}\right)-\beta\right\}
\end{aligned} \tag{38}$$

Downloaded from jvc.sagepub.com at National Science Library CAS on February 27, 2011

where

$$\varphi(\tau) = r\tau + \psi(\tau). \tag{39}$$

Assuming $\dot{A}(t)$ and $\dot{\psi}(t)$ are slow variables and their average remains constant during one cycle justifies that we may substitute the right-hand sides of equations (37) and (38) with their integral over one period of oscillation:

$$\begin{aligned}
\dot{A}(\tau) &= \int_0^{2\pi} \frac{1}{r}\dot{A}(\tau)d\varphi = -\pi\left[2\sqrt{2\alpha\beta}\,(1+2A_0)\ \sin[\psi(\tau)]\right. \\
&+ \left. A(\tau)\left\{\left(h + \frac{\pi a_6 r}{1+r^2}\right)r + \beta\sin[2\psi(\tau)]\right\}\right]
\end{aligned} \tag{40}$$

$$\begin{aligned}
\dot{\psi}(\tau) &= \int_0^{2\pi} \frac{1}{r}\dot{\psi}(\tau)d\varphi = \pi\left[A(\tau)\left\{1 - r^2 - 2\alpha - 2\beta - \beta\cos^2[\psi(\tau)]\right\}\right. \\
&- \left.\frac{\pi a_7}{1+r^2} - 2\sqrt{2\alpha\beta}\,(1+2A_0)\ \cos[\psi(\tau)]\right].
\end{aligned} \tag{41}$$

At steady-state conditions, $A(\tau)$ and $\psi(\tau)$ must not vary in time. Therefore, the left-hand sides of equations (40) and (41) are zero at steady-state conditions, which provide the following set of coupled algebraic equations:

$$2\sqrt{2\alpha\beta}\,(1+2A_0)\ \sin[\psi(\tau)] + A(\tau)\left\{\left(h + \frac{\pi a_6 r}{1+r^2}\right)r + \beta\sin[2\psi(\tau)]\right\} = 0 \tag{42}$$

$$\begin{aligned}
&A(\tau)\left\{1 - r^2 - 2\alpha - 2\beta - \beta\cos^2[\psi(\tau)]\right\} - \frac{\pi a_7}{1+r^2} \\
&\qquad -2\sqrt{2\alpha\beta}\,(1+2A_0)\ \cos[\psi(\tau)] = 0.
\end{aligned} \tag{43}$$

Eliminating $\psi(\tau)$ provides a relationship between the parameters of the system to have a periodic steady-state response with frequency r

$$\begin{aligned}
&Z_1 r^{12} + Z_2 r^{10} + Z_3 r^9 + Z_4 r^8 + Z_5 r^7 + \left(Z_6 - Z_7\sqrt{Z_8}\right)r^6 \\
&+ Z_9 r^5 + \left(Z_{10} - Z_{11}\sqrt{Z_8}\right)r^4 + Z_{12}r^3 + \left(Z_{13} - Z_{11}\sqrt{Z_8}\right)r^2 \\
&+ Z_{14}r + Z_{15} - Z_{16}\sqrt{Z_8} = 0
\end{aligned} \tag{44}$$

where Z_i (indicated in Appendix A) are dynamic parameters of the system not related to the excitation frequency.

Note that the non-zero excitation command embedded in β is necessary to have a non-trivial response; however, the other parameters may be set to zero. The effect of variation of each parameter on the dynamic response of the MEMS will be examined in the next section. Although the system is analyzed in the linear approximate domain, the frequency response of the system is complicated and hard to utilize for manipulation. The effect of the

Downloaded from jvc.sagepub.com at National Science Library CAS on February 27, 2011

Table 1. Nominal values of the dynamic parameters of the MEMS.

M	1×10^{-11} kg
c	1×10^{-8} Nsm^{-1}
d	2.0 μm
α	0.0000553125 v_p^2
A	200×50 μm
β	0.00002765625 v_i^2

individual parameters is also not clear in the response equation of the system. Therefore, a numerical analysis is usually needed to evaluate the overall effect of the parameters. In what follows, the analytical description (44) is utilized to describe the behavior of the steady-state dynamics of the system around resonance.

In theory, equation (44) must be solved for A as a function of r

$$\frac{A}{2\sqrt{2\alpha\beta}\left(1+r^2\right)\left(1+2A_0\right)} = \frac{\sqrt{r^8+Z_{17}r^6+Z_{18}r^5+Z_{19}r^4+Z_{20}r^3+Z_{21}r^2+Z_{22}r+Z_{23}}}{r^8+Z_{24}r^6+Z_{18}r^5+Z_{25}r^4+Z_{26}r^3+Z_{27}r^2+Z_{28}r+Z_{29}}. \quad (45)$$

Then, the real root of $dA/dr = 0$ for r introduces a new equation for the resonant frequency r_0 as a function of the dynamic parameters h, α, a_6, a_7, and β. The equation can then be examined for determining the shift of resonant frequency in the effect of varying dynamic parameters numerically.

Because of the hard limit of collations, the peak value should be less than d, or less than one in dimensionless form. The design criteria for the electric actuated microcantilever resonator would be a relationship between dynamic parameters that produced a peak value equal to one. Keeping $A = 1$, a design surface in the parameter space $\alpha-\beta-h$ can be defined for a fixed value of a_6 and a_7. The design surface divides the parameter space into two (or more) sections, indicating a possible and impossible design half-space. A set of parameters on the surface corresponds to the limit values of design parameters.

5. RESULTS

Equation (44) describes the frequency behavior of the microresonator, indicating that its dynamics is governed by the polarization voltage parameter α, the alternative excitation voltage parameter β, the damping parameter h, the excitation frequency ratio r, as well as the thermal damping and stiffness parameters a_6, and a_7. In order to demonstrate the dependency of the steady-state behavior of the MEMS, we graphically illustrate the frequency response for various parameters. Table 1 indicates the nominal values of a sample microcantilever resonator to analyze the dynamic behavior of the MEMS, although, because of the dimensionless form of the equations, any other MEMS can be analyzed as well (Kanda et al., 2000; Yang et al., 2002; Khaled et al., 2003; Kaajakari et al., 2004).

Downloaded from jvc.sagepub.com at National Science Library CAS on February 27, 2011

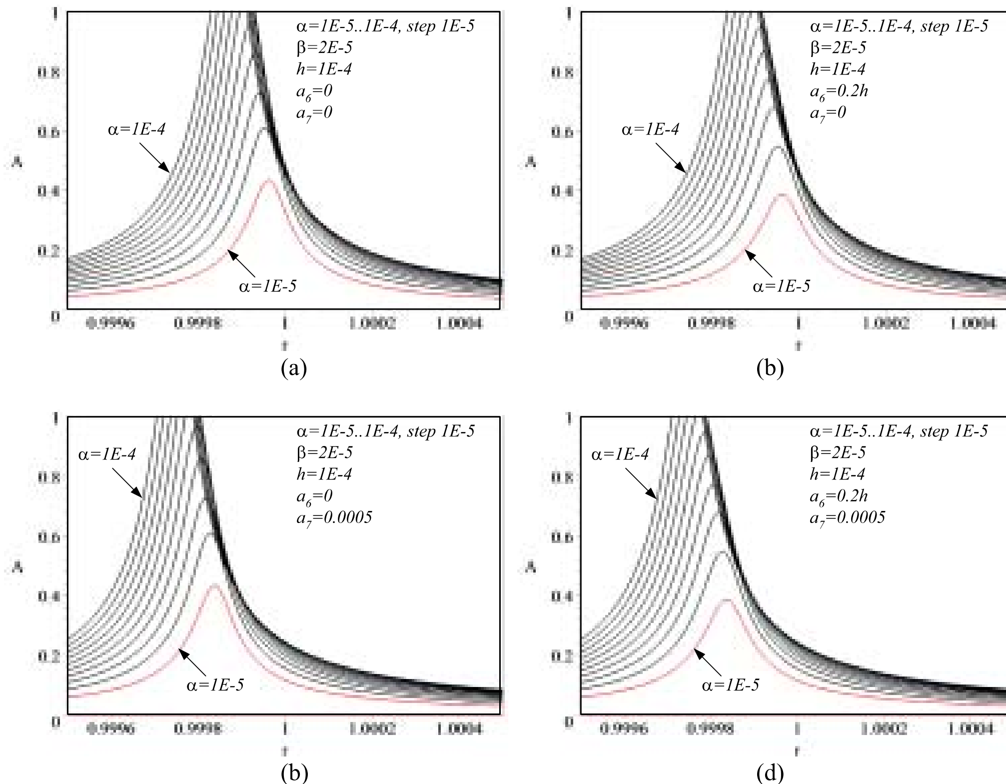

Figure 2. Effect of the variation of the polarization voltage on frequency response.

Figure 2 depicts the effect of the variation of the polarization voltage for a set of parameters. The amplitude of the steady-state oscillation increases by increasing the polarization voltage. No thermal effect is shown in Figure 2(a) where a_6 and a_7 are set to zero. Thermal damping increases the damping of the system near resonance, and hence diminishes the resonance amplitudes, but has almost no effect on the off-resonance responses, as shown in Figure 2(b). Thermal relaxation appears by non-zero a_7, which makes the microbeam softer. Softening of the microbeam shifts the resonance frequency to lower values. This effect, which is shown in Figure 2(c), is important for resonator mass sensors which have been analyzed and designed assuming constant stiffness. Figure 2(d) shows the frequency response of the microbeam with both effects: thermal damping and relaxation. The values of both thermal damping and thermal stiffness coefficients are set to 20% of the nominal values of the linear damping and stiffness of the system. As shown in Figure 2, the peak value of the frequency response at resonance is a monotonically increasing function of the polarization voltage, partially because of the effect of α on A_0. Therefore, there must be a maximum acceptable α, due to constraint $Y < 1$.

The response of the system to the variation of the excitation voltage has the same pattern as changing the polarization voltage (see Figure 3). More specifically, the peak value

Downloaded from jvc.sagepub.com at National Science Library CAS on February 27, 2011

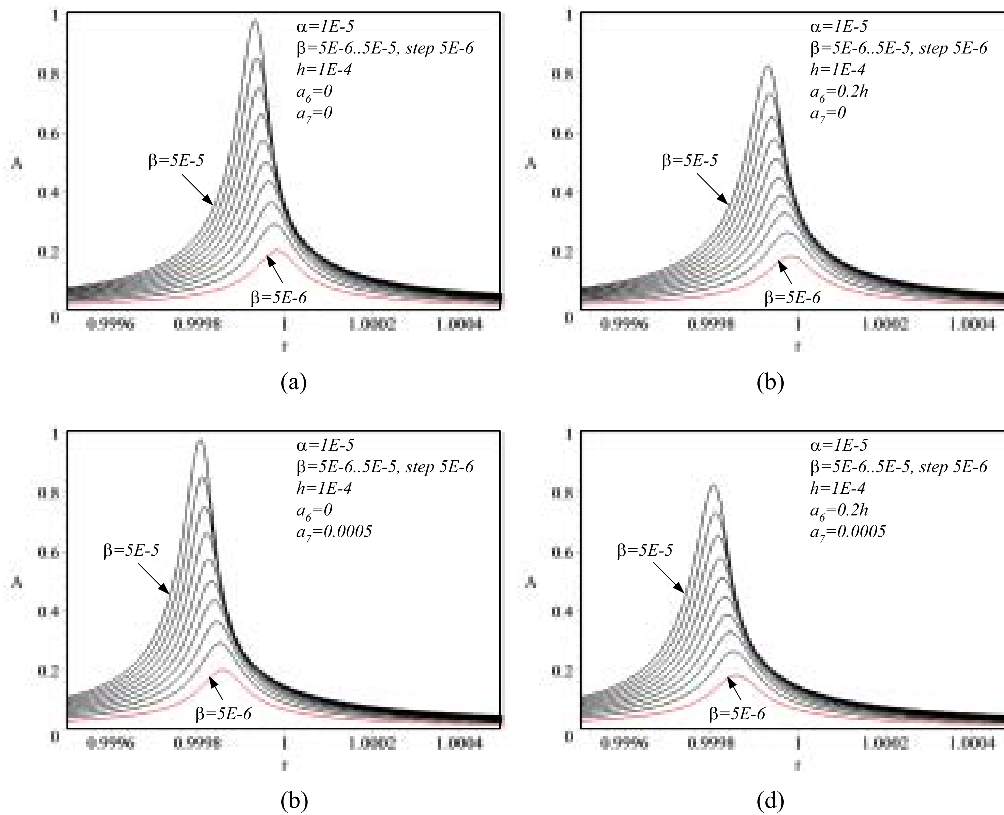

Figure 3. Effect of the variation of the excitation voltage on frequency response.

increases and the resonant frequency shifts to lower frequencies when the amplitude of the excitation voltage increases. Thermal damping and relaxation also have the same effects as described for polarization voltage variation. There is also a higher limit for the alternative voltage to have oscillation within the gap size limit.

The variation of the damping ratio is illustrated in Figure 4. Increasing the damping ratio diminishes the amplitude of the oscillation as expected. However, decreasing the damping increases the quality factor of the system and is not considered a positive phenomenon. Damping has two main roles in MEMS dynamics. It should exist to control the system to remain within the physical boundary $Y < 1$, and it must be as low as possible to provide a high quality factor.

Frequency response analysis has shown that the thermal relaxation has the most impact on resonance frequency shifting because of the direct effect of stiffness reflected in the primary natural frequency. However, polarization and excitation voltages also have a softening effect and shift the resonance frequency to lower values. Moreover, viscous and thermal dampings have the least effect on resonance frequency with high effects on decreasing the peak amplitudes.

Downloaded from jvc.sagepub.com at National Science Library CAS on February 27, 2011

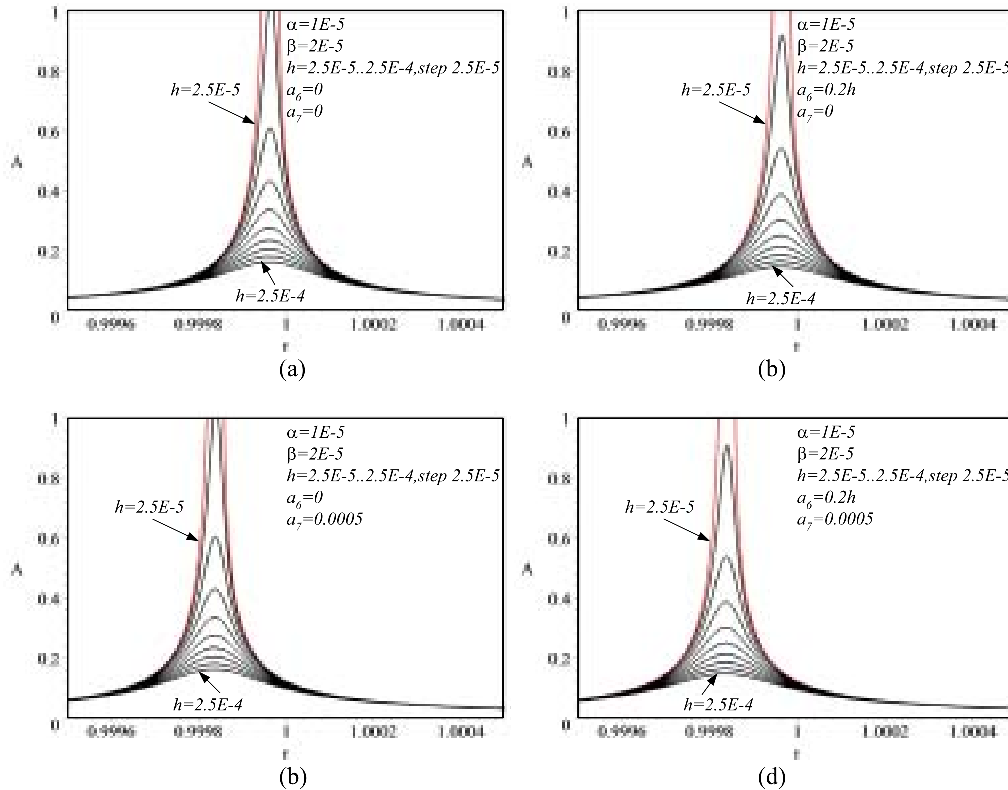

Figure 4. Effect of the variation of the damping ratio on frequency response.

Figure 5 depicts the effects of varying the thermal damping and stiffness coefficients on the frequency response of the microresonator. As shown in Figure 5(a), thermal damping mainly influences the peak amplitude at resonance and does not affect the off-resonant responses. This is also true when there is thermal relaxation (see Figure 5b). However, as shown in Figures 5(c) and (d), the effect of thermal relaxation appears in a resonance shift.

The resonance frequency of MEMS is a very important parameter, especially in resonator-based microsystems. The resonance frequency also determines the amount of force the structure can exert. In addition, the resonant frequency indirectly affects design parameters such as the quality factor, the switching frequency of MEMS, and the effects of external noise (Sudipo and Aluru, 2004). To determine the capability of the MEMS to sense a shift in resonance frequency by varying a parameter, equation (44) must be investigated numerically.

The shift of resonance frequency, r_0, is illustrated in Figures 6 and 7. First, the thermal coefficients a_6 and a_7 are set to zero and the result is shown in Figure 6(a). The resonance frequency is a monotonically decreasing function of increasing both polarization and excitation voltages, when the thermal effects are ignored. Within the limit of possible variation of voltages according to the physical limit of gap, the behavior of resonance shifting looks linear with variation of both voltages. This is also true when thermal effects are present; see

Downloaded from jvc.sagepub.com at National Science Library CAS on February 27, 2011

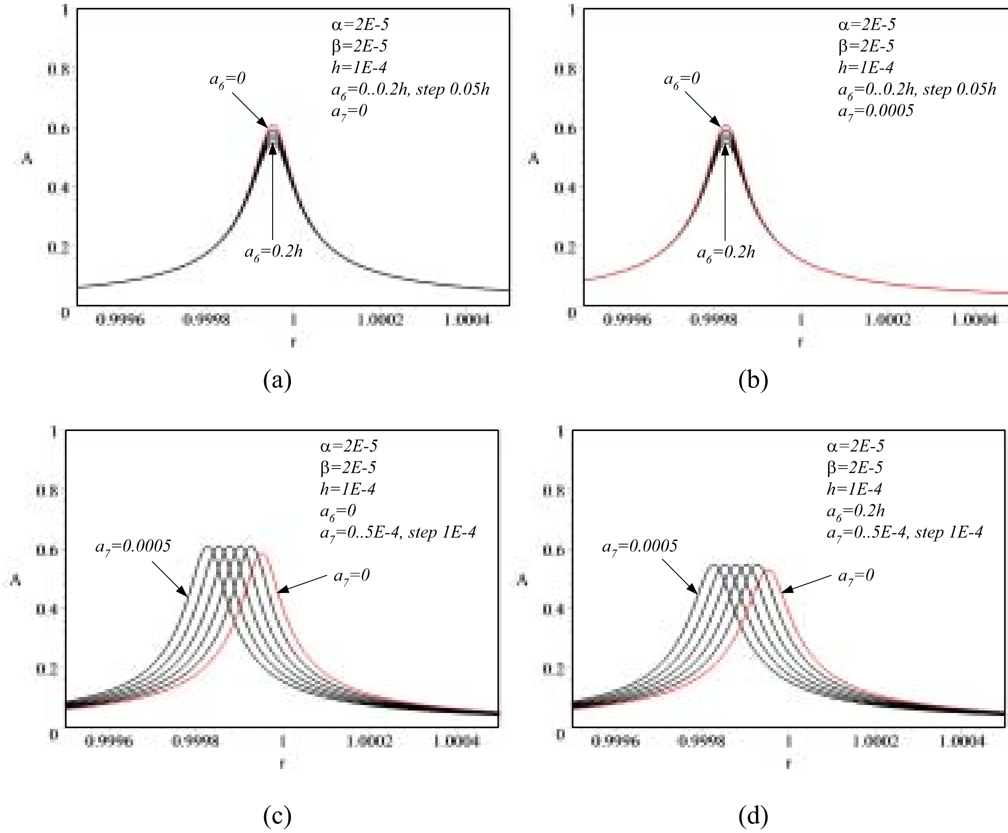

Figure 5. Effect of the variation of thermal damping and stiffness on frequency response.

Figures 6(b)–(d). A three-dimensional illustration is provided in Figure 6(e) to show this behavior better. As can be seen, increasing thermal damping increases the resonance frequency slightly; however, the resonance frequency deceases by increasing the temperature relaxation significantly.

The behavior of the resonant frequency is not linear or monotonic when damping is varied (Figure 7). Figure 7(a) depicts the effect of the variation of damping and polarization voltage on the resonant shift when the thermal effects are ignored. The resonance frequency is sensitive when damping is low. However, its sensitivity disappears shortly. Resonance frequencies are compared in Figures 7(b) and (c) for thermal damping and thermal relaxation, respectively. Note that a_6 and a_7 have opposite effects when damping is varied. However, the relaxation has a dominant effect, as indicated in Figure 7(d). The three-dimensional illustration in Figure 7(e) portrays this nonlinear behavior.

The peak value of the oscillation amplitude A_p at resonance is the second important sensible parameter of microresonators. The evaluation of the peak amplitude starts with searching numerically for the resonance frequency, which is the real root of equation (45). Upon having a resonance frequency, substitution back into equation (44) makes another implicit function to be solved for the peak amplitude. The results of these calculations are illustrated

Downloaded from jvc.sagepub.com at National Science Library CAS on February 27, 2011

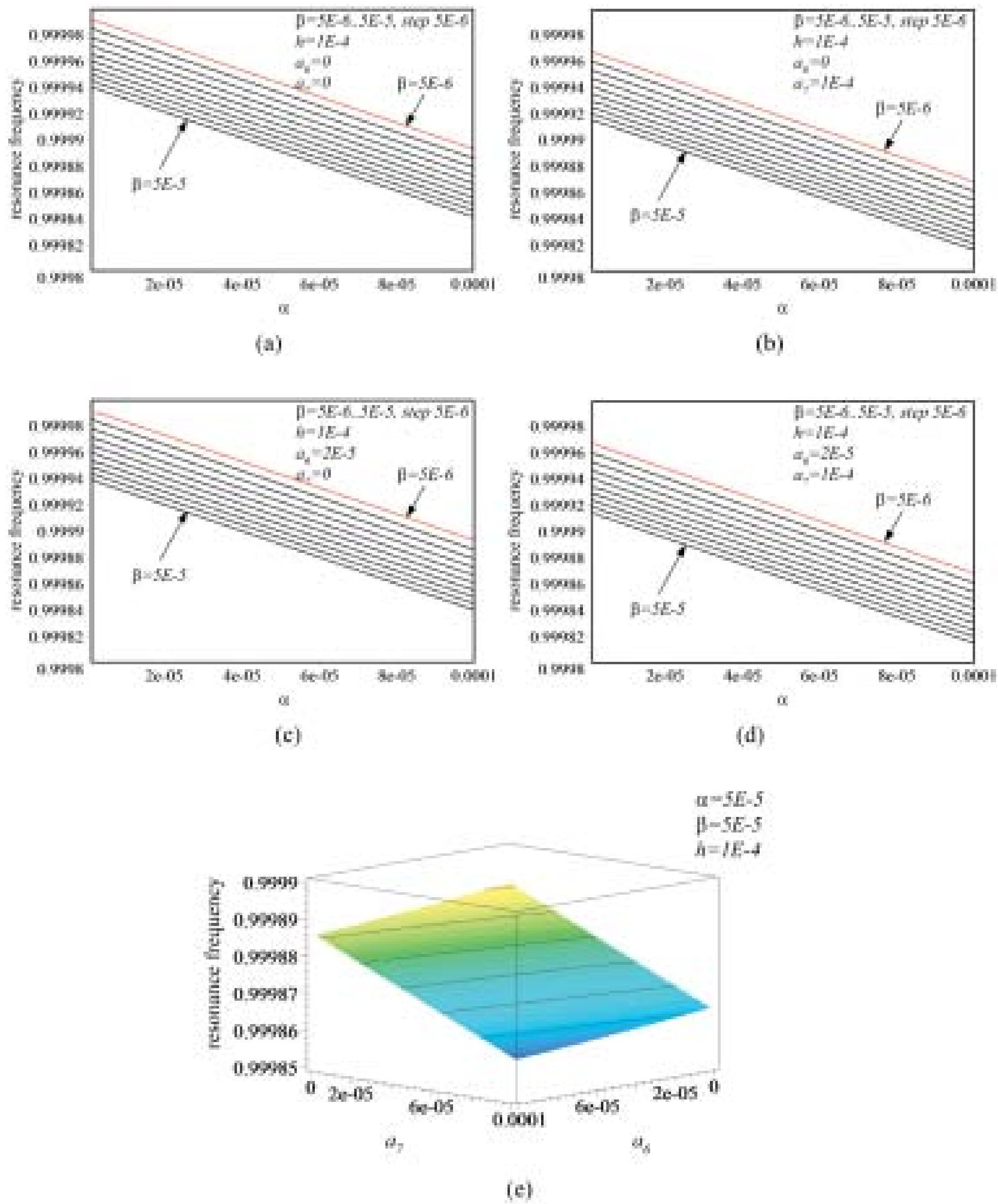

Figure 6. Effect of the variation of excitation and polarization voltages on the resonance shift.

in Figure 8. Comparing Figures 8(a)–(d) depicts how non-zero a_6 decreases the peak amplitudes slightly, while non-zero a_7 increases the peak amplitude. These effects are expected because a_6 directly increases the damping of the system at resonance, and a_7 decreases the stiffness of the system at resonance. A_p is a nonlinear monotonically increasing function of both polarization and excitation voltages, while it is a decreasing function of damping.

Downloaded from jvc.sagepub.com at National Science Library CAS on February 27, 2011

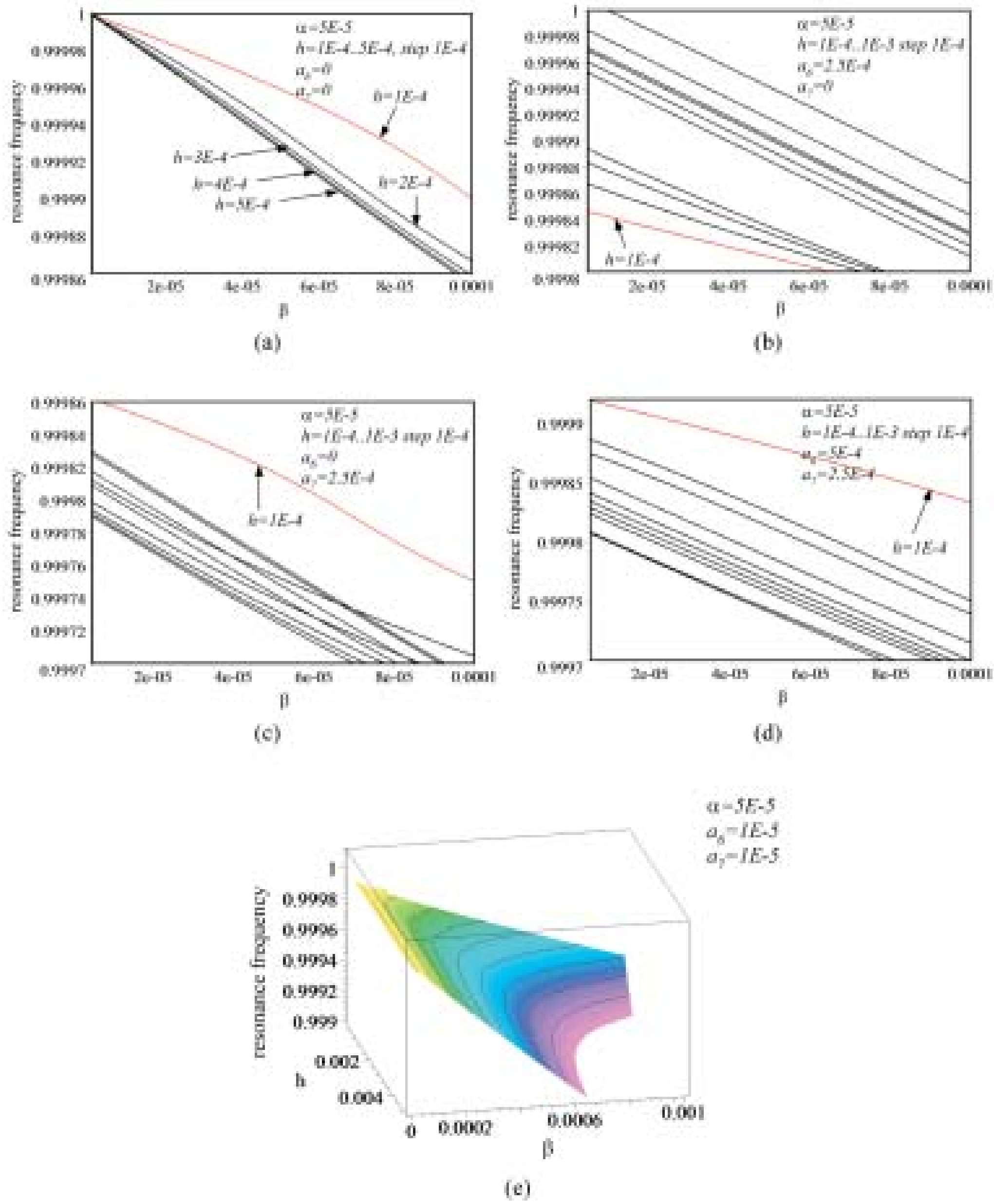

Figure 7. Effect of the variation of damping and excitation voltage on the resonance shift.

The effect of damping variation is only illustrated in a single figure for no thermal effects (Figure 9) because the behavior of the peak amplitude is qualitatively similar in the presence of the thermal effects. The peak amplitude is a monotonically decreasing function of damping.

Downloaded from jvc.sagepub.com at National Science Library CAS on February 27, 2011

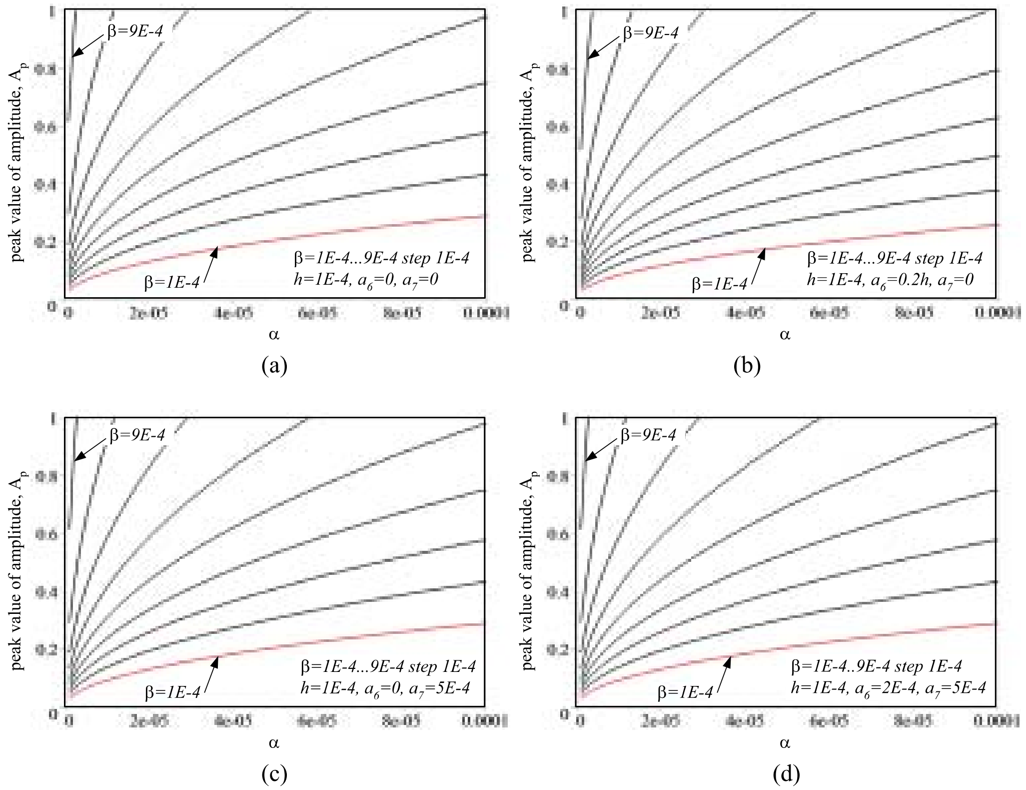

Figure 8. Effect of the variation of excitation and polarization voltages on the peak amplitude at resonance.

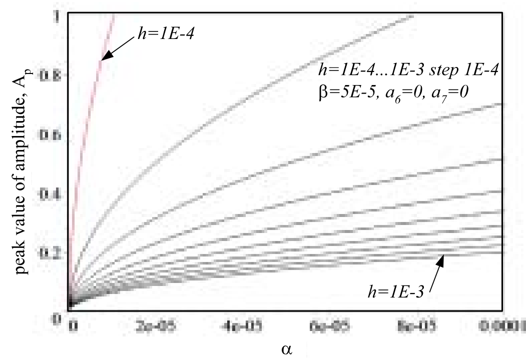

Figure 9. Effect of the variation of damping and polarization voltages on the peak amplitude at resonance.

Downloaded from jvc.sagepub.com at National Science Library CAS on February 27, 2011

6. CONCLUSION

We have modeled the thermal phenomena in microresonator dynamics. The thermal phenomena have been translated to effective forces per unit length of the vibrating microbeam. The thermal properties of the microbeam contribute to system damping as a result of warming and heat energy dissipation, and to system stiffness as a result of material heat softening. We have called the heat softening "temperature relaxation", to remind of the characteristic of stiffness change, and we have called heat loss "thermal damping" to denote its function. Both effects of thermal behavior are frequency-dependent. Analytical research has shown that the thermal damping and relaxation can be described by a suitable Lorentzian function. So, we have simulated the damping and stiffness effects using a Lorentzian function. The thermal damping force is positive while the thermal restoring force is negative, since the thermal damping dissipates energy and the thermal stiffness decreases the mechanical stiffness.

Utilizing a set of dimensionless variables, the general equation of flexural motion of microbeams has been derived including the modeling of thermal effects. The steady-state response of the system has been analyzed employing the averaging perturbation method. The frequency responses, the resonant frequency shifting and the peak amplitude of vibration have been investigated by varying dynamic parameters involved. Because of the Lorentzian function, the thermal damping and temperature relaxation affect the steady-state response of the system close to resonance only. Thermal damping has a reduction effect on the peak amplitude, while temperature relaxation increases the peak amplitude with a dominant effect. In addition, temperature relaxation shows a significant effect on the shift of resonance frequency to lower values. Resonance shifting is a very important phenomenon, especially in resonator-based sensors. It seems to be the most effective source of errors in resonant sensors which are designed based on constant stiffness assumption.

APPENDIX A: DESCRIPTION OF THE Z_i PARAMETERS

$$Z_1 = 4\beta^2 A^4 \quad \text{(A1)}$$

$$Z_2 = 4\beta^2 A^4 \left(4\beta + 2 + 4\alpha + h^2\right) \quad \text{(A2)}$$

$$Z_4 = 8\beta^2 A^4 \left(a_7 + h a_6\right) \quad \text{(A3)}$$

$$\begin{aligned} Z_4 &= 4\beta^2 A^4 \left[\left(a_6 - 1 + 42\alpha + 4h^2 + 4\alpha^2\right) + \beta\left(3\beta + 8\alpha + 12\right)\right] \\ &- 16\alpha\beta^3 A^2 \left[4A_0\left(A_0 + 1\right) + 1\right] \end{aligned} \quad \text{(A4)}$$

$$Z_5 = 8\beta^2 A^4 \left[2a_7\left(\alpha + 1\right) + 3h a_6\right] \quad \text{(A5)}$$

$$\begin{aligned} Z_6 &= 4\beta^2 A^4 \left[8\alpha\left(\alpha + 1\right) + 2\left(3h^2 - 2\right) + 2a_6^2 + a_7^2\right] \\ &- 64\alpha\beta^3 A^2 \left[4A_0\left(A_0 + 1\right) + 1\right] \end{aligned} \quad \text{(A6)}$$

$$Z_7 = 16\beta^2 A^2 \left(A_0 + 1\right) \quad \text{(A7)}$$

$$Z_8 = \alpha\beta^2\left(1 + r^2\right)\left\{\alpha\left(2A_0 + 2\right) - A^2\left[\left(1 + r^2\right)\left(\beta + 2\alpha\right) + r\left(a_7 + r^3\right) - 1\right]\right\} \quad \text{(A8)}$$

$$Z_9 = 24\beta^2 A^4 \left[2a_7\left(\beta + \alpha\right) + h a_6\right] \quad \text{(A9)}$$

Downloaded from jvc.sagepub.com at National Science Library CAS on February 27, 2011

$$Z_{10} = 4\beta^2 A^4 \left\{\beta^3 [18\beta + 8(6\alpha - 1)] + 8\alpha(2\alpha - 1) + 4h^2 - 1 + a_6^2 + 2a_7^2\right\} - 96\alpha\beta^3 A^2 [4A_0(A_0 + 1) + 1] \tag{A10}$$

$$Z_{11} = 48\beta^2 A^2 (2A_0 + 1) \tag{A11}$$

$$Z_{12} = 8\beta^2 A^4 [4a_7(\beta + \alpha) + ha_6 - 2a_7] \tag{A12}$$

$$Z_{13} = 4\beta^2 A^4 \left\{\beta^2 [12\beta + 4(8\alpha - 3)] + 4\alpha(4\alpha - 3) + h^2 + 2 + a_7^2\right\} - 64\alpha\beta^3 A^2 [4A_0(A_0 + 1) + 1] \tag{A13}$$

$$Z_{14} = 8\beta^2 A^4 a_7 [2(\beta + \alpha) - 1] \tag{A14}$$

$$Z_{15} = 4\beta^2 A^4 \{\beta [4\beta + 4(2\alpha - 1)] + 4\alpha(\alpha - 1) + 1\} - 16\alpha\beta^3 A^2 [4A_0(A_0 + 1) + 1] \tag{A15}$$

$$Z_{16} = \frac{Z_{11}}{3} \tag{A16}$$

$$Z_{17} = 2\beta + 4\alpha + h^2 \tag{A17}$$

$$Z_{18} = 2\left(a_7 + a_6 h^2\right) \tag{A18}$$

$$Z_{19} = (2\alpha + \beta)(2\alpha + \beta + 2) + a_6^2 + 2h^2 - 2 \tag{A19}$$

$$Z_{20} = 2[a_6 h + a_7(2\alpha + \beta)] \tag{A20}$$

$$Z_{21} = (2\alpha + \beta - 1)^2 + a_7^2 + h^2 \tag{A21}$$

$$Z_{22} = 2a_7(2\alpha + \beta - 1) \tag{A22}$$

$$Z_{23} = (2\alpha + \beta - 1)^2 + 1 \tag{A23}$$

$$Z_{24} = Z_{17} + 2\beta \tag{A24}$$

$$Z_{25} = Z_{19} + 2\beta(1 + 2\alpha) \tag{A25}$$

$$Z_{26} = Z_{20} + 2a_7\beta \tag{A26}$$

$$Z_{27} = Z_{21} + 2\beta(4\alpha + 2\beta - 1) \tag{A27}$$

$$Z_{28} = Z_{22} + 2\beta a_7 \tag{A28}$$

$$Z_{29} = Z_{23} + 2\beta(2\alpha + \beta - 1). \tag{A29}$$

REFERENCES

Abdolvand, R., Ho, G. K., Erbil, A., and Ayazi, F., 2003, "Thermoelastic damping in ternech-refilled polysilicon resonators," in *Proceedings of the 12th International Conference on Solid State Sensors, Actuators and Microsystems*, Boston, MA, June 8–12.

Alblas, J. B., 1961, "On the general theory of thermoelastic friction," *Applied Science Research* **A10**, 349–362.

Alblas, J. B., 1981, "A note on the theory of thermoelastic damping," *Journal of Thermal Stresses* **4**, 333–355.

Downloaded from jvc.sagepub.com at National Science Library CAS on February 27, 2011

Barmatz, M. and Chen, H. S., 1974, "Young's modulus and friction in metallic glass alloys from 1.5 to 300 K," *Journal of Physical Review B* **9(10)**, 4073–4083.

De, S. K. and Aluru, N. R., 2004, "Full-Lagrangian schemes for dynamic analysis of electrostatic MEMS," *Journal of Microelectromechanical Systems* **11(5)**, 737–758.

Fejer, M. M., Rowan, S., Cagnoli, G., Crooks, D. R. M., Gretarsson, A., Harry, G. M., Hough, J., Penn, S. D., Sneddon, P. H., and Vyatchanin, S. P., 2004, "Thermoelastic dissipation in inhomogeneous media: loss measurements and displacement noise in coated test masses for interferometric gravitational wave detectors," *Physical Review D* **70**, 082003.

Gough, W., 1968, "The graphical analysis of a Lorentzian function and a differentiated Lorentzian function," *Journal of Physical Review A* **2(1)**, 704–709.

Gysin, U., Rast, S., Meyer, E., Lee, D. W., Vettiger, P., and Gerber, C., 2004, "Temperature dependence of the force sensitivity of silicon cantilevers," *Physical Review B* **69**, 045403, 1–6.

Hsu, T. R., 2002, *MEMS and Microsystems Design and Manufacture*, MGraw Hill, New York.

Hsu, W. T., Clark, J. R., and Nguyen, C. T, 2001, "Q-optimized lateral free-free beam micromechanical resonators," in *Proceedings of the 11th International Conference on Solid-State Sensors and Actuators (Transducers '01)*, Munich, Germany, pp. 1110–1113.

Husman, M. E., Hough, J., and Robertson, N. A., 2004, "Thermal noise in a pendulum suspended by multiple wires," *Classical Quantum Gravity* **21**, 1371–1381.

Jeong, J., Chung, S., Lee, S. H., and Kwon, D., 2003, "Evaluation of elastic properties and temperature effects in Si thin film using an electrostatic microresonator," *Journal of Microelectromechanical Systems* **12(4)**, 524–530.

Kaajakari, V., Mattila, T., Oja, A., and Seppä, H., 2004, "Nonlinear limits for single-crystal silicon microresonators," *IEEE Journal of Microelectromechanical Systems* **13(5)**, 715–724.

Kanda, T., Morita, T., Kurosawa, M. K., and Higuchi, T., 2000, "A flat type touch probe sensor using PZT thin film vibrator," *Sensors and Actuators* **83**, 67–75.

Karami, G. and Garnich, M., 2005, "Micromechanical study of thermoelastic behavior of composites with periodic fiber wariness," *Journal of Composites B* **36**, 241–248.

Khaled, A. R. A., Vafai, K., Yang, M., Zhang, X., and Ozkan, C. S., 2003, "Analysis, control and augmentation of microcantilever deflections in bio-sensing systems," *Sensors and Actuators B* **94**, 103–115.

Lifshitz, R. and Roukes, M. L., 2000, "Thermoelastic damping in micro- and nanomechanical systems," *Physical Review* **61(8)**, 5600–5609.

Meirovitch, L., 1997, *Principles and Technologies of Vibrations*, Prentice-Hall, Englewood Cliffs, NJ.

Nayfeh, A. H. and Younis, M. I., 2004, "A new approach to the modeling and simulation of flexible microstructures under the effect of squeeze-film damping," *Journal of Micromechanics and Microengineering* **14**, 170–181.

Nguyen, C. T. C., 1995, "Micromechanical resonators for oscillators and filters," in *Proceedings of the IEEE International Ultrasonic Symposium*, Seattle, WA, November 7–10, pp. 489–499.

Norris, A. N. and Photiadis, D. M., 2005, "Thermoelastic relaxation in elastic structures, with applications to thin plates," *Quarterly Journal of Mechanics and Applied Mathematics* **58(1)**, 145–163.

Saulson, P. R., 1990, "Thermal noise in mechanical experiments," *Physical Review D* **42(8)**, 2437–2445.

Srikar, V. T. and Senturia, S. D., 2002, "Thermoelastic damping in fine-grained polysilicon flexural beam resonators," *Journal of Microelectromechanical Systems* **11(5)**, 499–504.

Sudipo, K. and Aluru, N. R., 2004, "Full-Lagrangian schemes for dynamic analysis of electrostatic MEMS," *Journal of Microelectromechanical Systems* **13(5)**, 737–758.

Wang, K., Wong, A. C., and Nguyen, C. T., 2000, "VHF free–free beam high-Q micromechanical resonators," *Journal of Microelectromechanical Systems* **9**, 347–360.

Yang, J. L., Ono, T., and Esashi, M., 2002, "Energy dissipation in submicrometer thick single-crystal silicon cantilevers," *Journal of Microelectromechanical Systems* **11**, 775–783.

Yasymura, K. Y., Stowe, T. D., Chow, E. M., Pfafman, T., Kenny, T. M., Stipe, B. C., and Rugar, D., 2000, "Quality factors in micron- and submicron-thick cantilevers," *Journal of Microelectromechanical Systems* **9(1)**, 117–125.

Younis, M. I., 2004, "Modeling and Simulation of Microelectromechanical System in Multi-Physics Fields," Ph.D. Thesis, Engineering Science and Mechanics, Virginia Polytechnic Institute and State University Blacksburg, VA.

Younis, M. I. and Nayfeh, A. H., 2003, "A study of the nonlinear response of a resonant microbeam to electric actuation," *Nonlinear Dynamics* **31**, 91–117.

Downloaded from jvc.sagepub.com at National Science Library CAS on February 27, 2011

Younis, M. I., Abdel-Rahman, E. M., and Nayfeh, A. H., 2003, "A reduced-order model for electrically actuated microbeam-based MEMS," *Journal of Microelectromechanical Systems* **12(5)**, 672–680.

Zalalutdinov, V., Mattila, T., Oja, A., and Seppa, H., 2004, "Nonlinear limits for single-crystal silicon microresonators," *Journal of Microelectromechanical Systems* **13(5)**, 715–724.

Zener, C., 1937, "Internal friction in solids: I. Theory of internal friction in reeds," *Physical Review* **52**, 230–235.

Zener, C., 1938a, "Internal friction in solids: II. General theory of thermoelastic internal friction," *Physical Review* **53**, 90–99.

Zener, C., 1938b, "Internal friction in solids: IV. Relation between cold work and internal friction," *Physical Review* **53**, 582–586.

Zener, C., 1948, *Elasticity and Anelasticity of Metals*, University of Chicago Press, Chicago, IL.

Zener, C., Otis, W., and Nuckolls, R., 1938, "Internal friction in solids: III. Experimental demonstration of thermoelastic internal friction," *Physical Review* **53**, 100–101.

Downloaded from jvc.sagepub.com at National Science Library CAS on February 27, 2011